Low genetic variation is associated with low mutation rate in the giant duckweed

Shuqing Xu[1,2*], Jessica Stapley[2], Saskia Gablenz[3], Justin Boyer[3], Klaus J. Appenroth[4], K. Sowjanya Sree[5], Jonathan Gershenzon[3], Alex Widmer[6] and Meret Huber[3,7*]

Affiliations:

[1]Institute of Evolution and Biodiversity, University of Münster, Hüfferstrasse 1, 48149 Münster, Germany.

[2]Center for Adaptation to a Changing Environment, ETH Zurich, Universitätstrasse 16, 8092 Zürich, Switzerland.

[3]Department of Biochemistry, Max Planck Institute for Chemical Ecology, Hans-Knöll-Strasse 8, 07745 Jena, Germany.

[4]Matthias-Schleiden-Institute, Plant Physiology, Friedrich Schiller University of Jena, Dornburgerstraße 159, 07743 Jena, Germany.

[5]Department of Environmental Science, Central University of Kerala, Periye 671316, India.

[6]Institute of Integrative Biology, ETH Zurich, Universitätstrasse 16, 8092 Zürich, Switzerland.

[7]Institute of Plant Biology and Biotechnology, University of Münster, Schlossplatz 7-8, 48143 Münster, Germany.

*Correspondence to: Shuqing Xu: shuqing.xu@uni-muenster.de or Meret Huber: huberm@uni-muenster.de

Abstract:

Mutation rate and effective population size (N_e) jointly determine intraspecific genetic diversity, but the role of mutation rate is often ignored. We investigate genetic diversity, spontaneous mutation rate and N_e in the giant duckweed (*Spirodela polyrhiza*). Despite its large census population size, whole-genome sequencing of 68 globally sampled individuals revealed extremely low within-species genetic diversity. Assessed under natural conditions, the genome-wide spontaneous mutation rate is at least seven times lower than estimates made for other multicellular eukaryotes, whereas N_e is large. These results demonstrate that low genetic diversity can be associated with large-N_e species, where selection can reduce mutation rates to very low levels, and accurate estimates of mutation rate can help to explain seemingly counter-intuitive patterns of genome-wide variation.

Running title: Low mutation rate in a tiny plant

One Sentence Summary: The low-down on a tiny plant: extremely low genetic diversity in an aquatic plant is associated with its exceptionally low mutation rate.

Main Text

Explaining within-species genetic diversity—measured as the level of intraspecific DNA sequence variation—is a major goal in evolutionary and conservation biology, as this diversity can influence how species cope with changing environments (*1*, *2*). While intraspecific genetic diversity is known to vary widely among species, the underlying causes remain controversial (*3*, *4*). According to population genetic theory, the population mutation parameter (θ) is determined by the product of the spontaneous neutral mutation rate (μ) and effective population size (N_e), and in diploid species $\theta = 4 \times N_e \times \mu$ (*5*). In practice, the parameter θ is often estimated by the average pairwise nucleotide diversity (π) at putatively neutral sites (*6*). While the role of N_e in explaining variation in genetic diversity among taxa has received much theoretical and empirical attention (*3, 4, 7*), the influence of variation in mutation rate and the interaction between N_e and mutation rate remain largely unknown.

As most spontaneous mutations are deleterious, selection should favor lower mutation rates, but in small populations the efficacy of selection to lower the mutation rate is limited as genetic drift overrides the effect of natural selection. This 'drift-barrier' hypothesis can explain variation in mutation rates and the observed negative relationship between effective population size and mutation rate among species (*8*). However, one counter-intuitive prediction of the drift-barrier hypothesis is that populations with large N_e may also have low genetic diversity if natural selection has driven mutation rates to very low levels. Whether this pattern is present in eukaryotes is unknown, largely due to the paucity of studies quantifying both genome-wide diversity and spontaneous mutation rates under natural conditions in organisms with different life histories and reproductive strategies.

To better understand the relationship between genetic diversity, mutation rate and N_e, we independently obtained genome- and range-wide estimates of genetic diversity and mutation rate in the diploid freshwater plant *Spirodela polyrhiza* L. (Schleid.) ('duckweed'; Lemnaceae). This species is one of the fastest growing angiosperms; under suitable growth conditions, it reproduces predominantly by asexual budding with a duplication rate of 2-3 days (*9, 10*). Consequently, *S. polyrhiza* often achieves extremely high census population sizes in nature as millions of individuals can be found in a single pond. However, previous studies using a limited number of genetic markers found low genetic diversity (*11, 12*).

To provide genome- and range-wide estimates of genetic diversity in *S. polyrhiza*, we resequenced the genomes of 68 genotypes representing the global distribution of the species, using Illumina short-read sequencing with 29X average coverage (Table S1). All sequence reads were aligned to the *S. polyrhiza* reference genome (*14*) using the BWA-MEM aligner and genetic variants were identified using GATK (*15*). In total, we found 996,115 biallelic and 7,880 multiallelic high-quality single nucleotide polymorphisms (SNPs) as well as 214,262 small indels. This represents on average one SNP per 145 bp in the *S. polyrhiza* genome, which is low compared to an average of 1 SNP per 23 bp in *Arabidopsis thaliana* when a comparable number of genotypes are sequenced (*16*). Among all biallelic SNPs, 14,191 nonsynonymous and 8,865 synonymous SNPs were found (Table S2 and External Dataset 1). The estimated *S. polyrhiza* range-wide pairwise nucleotide diversity at synonymous sites (π_s) was 0.00086, which is among the lowest values reported for any multicellular eukaryote for which genome-wide genetic diversity has been estimated (Table S3) (*3*).

Population structure analysis based on genome-wide polymorphisms revealed four population clusters in *S. polyrhiza*, which are centered in four geographic regions: America,

Europe, India and South East (SE) Asia (Figure 1). A few samples showed discrepancies between their geographic origin and population cluster assignment based on their genomic variation, likely due to either recent migrations of the duckweed associated with human activities or mis-labeling during long-term maintenance of the duckweed collections. The pairwise F_{st}, an indicator of relative differentiation between populations, ranged from 0.35 to 0.79 (Table S4), suggesting distinct regional populations in *S. polyrhiza*. Between populations, the genome-wide nucleotide diversity from all sites ranged between 0.00067 (SE Asian versus European population) and 0.00013 (European versus American population). Within populations, π calculated from all sites ranged from 0.00018 (American population) to 0.00056 (SE Asian population) (Table S5). The extent of linkage disequilibrium (LD), measured as the average distance between variants when their correlation coefficient (r^2) = 0.2, varied from 14.1 kb in the SE Asian population to 143.2 kb in the European population. The relatively slow decay of LD in *S. polyrhiza* may be attributed to its predominantly clonal reproduction. Comparing across populations, we observed much faster LD decay in the SE Asian population, suggesting more frequent (historical or ongoing) sexual reproduction in this region and/or higher N_e. Together, these results establish that genome-wide nucleotide diversity in *S. polyrhiza* is extremely low and sexual reproduction might be more frequent in the SE Asian population.

To investigate if the observed low genomic diversity in *S. polyrhiza* can be explained by universally low mutation rate or, alternatively, low effective population size, we estimated the spontaneous mutation rate and used our estimates of mutation rate and genomic diversity to estimate effective population size. Mutation rates can be markedly affected by outdoor environmental stresses such as temperature fluctuations and ultraviolet (UV) light (*17-21*), conditions that prevail in the native habitats of *S. polyrhiza*. Consequently, we estimated the

105 genomic mutation rate in indoor and outdoor mutation accumulation (MA) experiments, and
106 manipulated UV light in the outdoor experiments to further assess the effect of environmental
107 stresses (Figure S1 and External Dataset 2). Offspring of a single common ancestor were
108 propagated as single descendants under these conditions for 20 generations (Figure S2), after
109 which individual plants from five replicates per treatment were collected, and their genomes
110 sequenced and compared to the ancestral genome. We obtained genome information for 16
111 individuals (including the common ancestor) with an average coverage of 28X (Table S6) and
112 identified genetic variants in more than 79.7% of the *S. polyrhiza* genome (~126 Mb). Among
113 the 15 offspring, four *de novo* mutations were identified and confirmed by Sanger sequencing.
114 These mutations all originated from the outdoor MA experiments, and located in non-coding
115 regions. One mutation (C:G->T:A) was found in a UV-shielded line and the other three
116 mutations (two C:G->T:A and one C:G->A:T) were found in UV-exposed lines (Table 1).
117 Further analysis that compared the heterozygous sites of maternal and offspring individuals
118 suggested a low false-negative rate for our mutation identification pipeline (1.6 ± 0.7%). Given
119 that the protein-coding region of the *S. polyrhiza* genome is 17.4 Mb, we estimate the number of
120 mutations per generation in the entire protein-coding DNA of *S. polyrhiza* under natural, outdoor
121 conditions to be 0.0042 ± 0.0038. As so few mutations were observed, we were unable to
122 perform robust statistical analysis. However, the higher number of mutations found in outdoor
123 samples and in the presence of UV light is consistent with the hypothesis that outdoor stresses
124 increase the spontaneous mutation rate.

125 The genome-wide mutation rate in *S. polyrhiza* is within the range of mutation rates
126 reported for unicellular eukaryotes and Eubacteria, but is more than seven times lower than the
127 reported rates for multicellular eukaryotes (Figure 2). This estimated seven-fold difference

between *S. polyrhiza* and other multicellular eukaryotes is a conservative estimate, as all MA experiments in other organisms were performed under controlled indoor conditions, which likely resulted in lower mutation rate estimates. Based on these independent estimates of genetic diversity and mutation rate, we can estimate N_e in *S. polyrhiza*. Assuming that mutation rates during the clonal and sexual reproduction phases of *S. polyrhiza* are equal, the estimated effective population size of *S. polyrhiza* is 9.0×10^5, which is among the highest estimates for multicellular eukaryotes (Table S3).

This relatively large N_e may have contributed to the evolution of a low mutation rate in *S. polyrhiza*, as selection can effectively drive down the mutation rate in populations with large N_e (*8*). In addition to large N_e, clonal reproduction in *S. polyrhiza* might have contributed to the evolution of a low mutation rate. In diploid species, natural selection mainly acts against deleterious homozygous variants, which appear after recombination during sexual reproduction (*22*). During the clonal phase, recessive deleterious mutations will accumulate as heterozygotes with little fitness effects. In the sexual phase these accumulated mutations can appear as homozygotes and will subsequently experience strong purifying selection. Therefore, for species such as *S. polyrhiza* that reproduce both clonally and sexually, the frequency of asexual reproduction may be negatively correlated with the mutation rate. As ~80% of all angiosperms (*23*), including many crop species (*24*), can reproduce clonally, variation in the frequency of sex may have large effects on the evolution of mutation rates in plants and contribute to variation in intraspecific genetic diversity among species.

A seemingly counter-intuitive prediction of the drift-barrier hypothesis is that populations with large N_e can exhibit low genetic diversity, provided that mutation rate has evolved to be very low. The results presented here on *S. polyrhiza* support this prediction. The role of mutation

rate in driving variation in genetic diversity has been largely ignored, because obtaining accurate estimates of genome-wide genetic diversity and spontaneous mutation rate in a range of organisms has been difficult in the past. Our study reveals that the low genomic diversity in *S. polyrhiza* largely stems from a low mutation rate and emphasizes that accurate estimates of mutation rates are important explaining patterns of genetic diversity within species.

Materials and Methods

Mutation accumulation experiments with *S. polyrhiza*

We performed a mutation accumulation (MA) experiment with *S. polyrhiza* for 20 generations. *Spirodela polyrhiza* plants were propagated under three conditions: i) indoors in the absence of UV light, ii) outdoors in the absence of natural UV light, and iii) outdoors in the presence of natural UV light. *Spirodela polyrhiza* genotype 7498 was pre-cultivated for three weeks in N-medium - which supports optimal growth (N-medium: 0.15 mM KH_2PO_4, 1 mM $Ca(NO_3)_2$ x 4 H_2O, 8 mM KNO_3, 5 µM H_3BO_3, 13 µM $MnCl_2$ x 4 H_2O, 0.4 µM Na_2MoO_4 x 2 H_2O, 1 mM $MgSO_4$ x 7 H_2O, 25 µM FeNaEDTA) - in a climate chamber operating under the following conditions: 16h light, 8h dark; light supplied by vertically arranged neon tubes (OSRAM, Lumilux, cool white L36W/840) on each side; light intensity at plant height: 186±3 µmol s^{-1} m^{-2} outside polystyrene tubes and 142±3 µmol s^{-1} m^{-2} inside polystyrene tube; temperature: 28 °C constant; humidity: 41 %. The genotype 7498 originating from North Carolina (USA) was selected based on the existence of a clone-specific reference genome (*14*). A single frond (S1) was transferred to a transparent 50 ml polystyrene tube (28.5 x 95 mm, Kisker) containing 30 ml N-medium, covered with foam cap and incubated in a climate chamber under the above specified conditions. To obtain 6 MA lineages per treatment, the S1 ancestor was propagated according to the propagation scheme (Figure S2) every two to three days when

daughter fronds had fully emerged from the mother frond. For the indoor MA lines, 6 lineages were consequently propagated as single descendants for 20 generations under the same conditions as described above over a period of six weeks. For the outdoor MA lines, plants were moved at the end of June 2016 into a sun-exposed field site in Jena, Germany (50°53'06.7''N 11°40'53.1''E). The fronds were propagated in plastic beakers containing 180 ml N-medium that were fitted into the cavities of white polyvinyl chloride inserts (3 mm thickness) floating inside water-filled 10 L buckets. The buckets were surrounded with a 20 cm isolation layer of soil to avoid extreme temperature fluctuations and refilled with water to compensate for evaporating water whenever needed. To manipulate UV light, the buckets were covered with either UV transmitting (GS 2458, Sandrock, Germany) or UV blocking (UV Gallery100, Sandrock, Germany) Plexiglas plates with 1 – 3 cm distance between the bucket edge and the plates to allow air circulation. Each MA lineage was propagated in a separate bucket. After transplanting the fronds into the field, the buckets were shaded with two layers of green clear film for the first two days to allow plants to acclimate to outdoor conditions. The first green clear film layer was removed after two days, the second layer after four days. Plants were then propagated every two to four days for the following two months as single descendants for 20 generations. The MA lineages were randomized between the buckets every two weeks. The 20th generation of the outdoor plants was moved back to the original growth chamber. To obtain genomic DNA for whole genome re-sequencing (WGS), a single frond of the 20th generation of each of the indoor and outdoor MA lines and the ancestor, of which the roots and reproductive pockets were removed, was frozen in liquid nitrogen. All samples were stored at -80 °C until DNA extraction.

DNA isolation and whole genome resequencing

196 The plant tissue was ground by vigorously shaking the Eppendorf tubes with three metal
197 beads for 1 min in a paint shaker (Skandex S-7, Fluid Management, Sassenheim Holland) at 50
198 Hz. All DNA samples were isolated using the CTAB method (*25*) and their quantity and quality
199 was analyzed on Qubit. The DNA samples from the MA experiments were sequenced on
200 Illumina HiSeq 4000 at the Genomics Center of the Max Planck Institute for Plant Breeding
201 Research in Cologne (Germany) with 150 bp paired-end reads. For the 68 *S. polyrhiza*
202 genotypes, all genotypes of *Spirodela polyrhiza* (L.) Schleid. (listed in Table S1) were taken
203 from the stock collection of the Department of Plant Physiology, University of Jena, Germany.
204 Plants were then grown in N-medium (see details above) under a constant temperature of 28 °C
205 and 41% humidity. Detailed information and origin of the 68 *S. polyrhiza* genotypes is listed in
206 Table S1. The genomes of the 68 genotypes of *S. polyrhiza* were sequenced on Illumina HiSeq X
207 Ten at BGI (Shenzhen, China) with 150 bp paired-end reads. On average, 48.2 million reads per
208 genotype were generated.

209 **Short-read trimming, mapping and variant calling**

210 For all sequenced short reads, low-quality reads and adaptor sequences were trimmed
211 with AdapterRemoval v2.0 (*26*) with the parameters: --collapse --trimns --trimqualities –
212 minlength 36. All of the trimmed reads were then mapped to the *S. polyrhiza* reference genome
213 (*14*) using BWA-MEM (*27*) with default parameters. All reads with multiple mapping positions
214 in the genome were removed and only the mapped reads were kept. PCR duplicates were
215 removed using the "rmdup" function from SAMtools (*28*). The aligned reads were then used for
216 variant (SNPs and small indels) calling using GATK v3.5 (*15*) following the suggestions on best
217 practices (*29, 30*). In brief, the aligned reads around indels were re-aligned using
218 "IndelRealigner", and variants were called using the "UnifiedGenotyper" function with the

option "-stand_call_conf 30 -stand_emit_conf 10". The variants were then filtered with the option "'MQ0 >= 4 && ((MQ0 / (1.0 * DP)) > 0.1) & QUAL < 30.0 & QD < 5.0'". The variant clusters were further annotated as more than three variants within 50 bp using the GATK "VariantFiltration" function. Only biallelic loci were kept for downstream analysis. The synonymous and non-synonymous variants were annotated using snpEFF (version 4.3m) (*31*). Due to low sequencing coverage, three individuals from the MA experiments were removed from downstream analysis (Figure S2).

Population genomic analysis

To analyze genetic diversity and population genomics of the 68 genotypes, additional filtering steps "-s -f "DP > 510 & DP < 10200"" were performed using vcffilter (https://github.com/vcflib/vcflib#vcffilter). Loci with missing data, variants from mitochondrial and chloroplast regions and clustered variants were removed using vcftools (*32*). The population structure among the sequenced 68 genotypes was analyzed using fastSTRUCTURE v1.0 (*33*). Multiple K values (refers to number of populations) ranging from 1 to 10 were analyzed and the value K = 4 was selected using the chooseK.py function from the fastSTRUCTURE package. The genome-wide intra-specific diversity was analyzed using Popgenome v2.2.0 (*34*) and diversity at synonymous and non-synonymous sites was analyzed using SNPGenie (*35*). Plink (*36*) was used to calculate pairwise linkage disequilibrium (LD) from the dataset; related individuals were removed and only SNPs with minor allele frequency (MAF) greater than 0.05 were kept. To model the decline of LD with physical distance, pairwise r^2 between sites was used as the use of D´ is sensitive to small sample sizes (*37, 38*), and the decline of LD was modeled using Sved's equation: $E(r^2) = (1-/(1+4\ \beta d))+1/n$, where β is the decline in LD with distance d (*39*) and 1/n accounts for small sample size (*40*). The extent of useful LD for mapping

242 can be defined as $r^2 = 0.2$ (*41*). In this study we use mean r^2 for non-overlapping 100-bp bins to
243 fit Sved's equation.

244 **Mutation rate estimation and false-negative calculations**

245 Accurately estimating mutation rate requires a step-wise filtering and quality checking
246 process. The SNP filtering pipeline for the MA experiments was developed based on previous
247 studies (*42, 43*) and iterative manual inspections of the BAM files using Integrative Genomics
248 Viewer (IGV) (*44, 45*). 1) To reduce false positives, we only considered the mapped and
249 properly paired reads with insertion size greater than 100 bp and less than 600 bp using bamtools
250 (*46*). 2) We also excluded all genomic regions that were supported by fewer than nine or greater
251 than 75 reads per sample from both variant counting and genome size calculation, as the variants
252 from the regions that have low or high coverage are likely due to mapping errors (such as
253 repetitive or duplicated regions). On average, 79.7% of the genomic region was kept. 3) Because
254 spontaneous mutations should be only found in the offspring samples but not the ancestor, and
255 the likelihood of a mutation occurring at the exact same position in multiple samples is
256 extremely low (u^n, where u is the mutation rate, and n refers to number of samples), any variants
257 that appeared in more than two samples were removed. 4) Only the heterozygous variants that
258 were supported by at least three reads for both alleles were kept. After these filtering steps, 86
259 variants were found (Table S7). Among these, 56 were annotated as variant clusters, likely due to
260 mapping errors. To confirm this, we re-sequenced 28 of these variants that were located in
261 clusters using a Sanger sequencing approach and found none of them confirmed to be true
262 mutations. Therefore, all the variants that were classified as variant clusters were removed.

After removing all variant clusters, nine SNPs and 21 indels remained. Among the 21 indels, all of them were loss of heterozygosity in either the ancestral or offspring samples. Inspecting the alignment using the IGV showed that 19 of them were located in regions of simple sequence repeats or transposable elements, which were likely false positives. To confirm this, we selected 11 indels for Sanger sequencing and found that all of them were indeed false positives. As a result, all 21 indels were removed from the downstream analysis. Among the nine SNPs, six were point mutations (due to spontaneous mutations) and three were loss of heterozygosity (LOH) mutations (potentially due to gene conversion events). We further validated these SNPs using a Sanger-sequencing approach. Two LOH loci were very close to the gap of the genome assembly and the PCR primers could thus not be designed. We validated the remaining seven loci (six point mutations and one loss of heterozygosity). In total, four out of the six point-mutations were confirmed, and the loss of heterozygosity mutation turned out to be a false positive. The confirmed point-mutations are listed in Table 1 and were used for calculating the spontaneous mutation rate.

The relatively stringent parameters in the variant filtering process theoretically could result in a high rate of false negatives. To control this, we further estimated the false negative rate using the sequence data. We first identified all high-quality heterozygous SNP loci (30,392) from the ancestor using the same filtering parameters (coverage between nine and 75, and at least three reads to support each of the reference and the alternative allele) and compared them with the heterozygous SNPs in the offspring using a custom script. In theory, all these variants should be found in the clonally produced offspring. Thus, the number of SNPs that could not be identified from the offspring was used to estimate the highest boundary of the false negative rate

from our sequencing and variant calling/filtering pipeline, as some of these cases could be a true loss of heterozygosity.

Variant validation using Sanger sequencing

Because the total amount of DNA from a single individual was limited, the variant validation was performed using the descendants of the ancestor and offspring individuals. Specifically, at the end of the MA experiments, one individual of each line was propagated for four more generations under indoor conditions, after which the plants were frozen in liquid nitrogen for subsequent variant validation.

To validate the candidate variants, DNA was isolated as described above. PCR primers were designed based on the 500 bp flanking sequences. The PCR reactions were performed with goTaq DNA polymerase (Promega) using 30 PCR cycles with an annealing temperature of 58°C. The primer information is listed in supplemental Table S8. The PCR products were checked on a 1.5% agarose gel. The PCR products were then used for sequencing reactions using BigDye v3.1, and the products from the sequencing reactions were purified and sequenced on an ABI 3130XL sequencer.

Acknowledgments: We thank Claudia Michel, Beatrice Arnold and Yuanyuan Song for their help in validating the variants from the MA experiments, Stefanie Schirmer for help with the MA experiment and DNA isolation, Daniel Veit for manufacturing the facilities for outdoor duckweed growth, Thomas Städler and Martin Schäfer for constructive discussions commenting on the manuscript. We are also grateful to Tobias Neumann for providing meteorological data. **Funding:** This work was supported by a Marie Curie Intra-European Fellowship (No: 328935 to SX), the Alfred and Anneliese Sutter-Stöttner Foundation (to SX and MH), the Center for Adaptation to a Changing Environment (ACE) at ETH Zurich (to SX, JS and AW) and the Max Planck Society. **Author contributions:** S. G., A. W. and M. H. performed the experiments, J. S., J. B. and S. X. performed data analysis, K. J. A. and K. S. S. contributed to the giant duckweed collections, A. W. and J. G. provided resources. M. H. and S. X. conceived and supervised the project, S. X. wrote the manuscript with input from all co-authors. **Competing interests:** The authors declare no competing interests. **Data and materials availability:** Processed data are available in the manuscript or the supplementary materials. All raw DNA sequences obtained in this study are submitted to NCBI under Bioproject PRJNA476302.

References:

1. J. Forcada, J. I. Hoffman, Climate change selects for heterozygosity in a declining fur seal population. *Nature* **511**, 462-465 (2014).
2. E. Vander Wal, D. Garant, M. Festa-Bianchet, F. Pelletier, Evolutionary rescue in vertebrates: evidence, applications and uncertainty. *Phil. Trans. R. Soc. Lond. B Biol. Sci.* **368**, 20120090 (2013).
3. J. Romiguier *et al.*, Comparative population genomics in animals uncovers the determinants of genetic diversity. *Nature* **515**, 261-263 (2014).
4. H. Ellegren, N. Galtier, Determinants of genetic diversity. *Nat. Rev. Genet.* **17**, 422-433 (2016).
5. G. A. Watterson, On the number of segregating sites in genetical models without recombination. *Theor. Popul. Biol.* **7**, 256-276 (1975).
6. F. Tajima, Evolutionary relationship of DNA sequences in finite populations. *Genetics* **105**, 437-460 (1983).
7. R. B. Corbett-Detig, D. L. Hartl, T. B. Sackton, Natural selection constrains neutral diversity across a wide range of species. *PLoS Biol.* **13**, e1002112 (2015).
8. W. Sung, M. S. Ackerman, S. F. Miller, T. G. Doak, M. Lynch, Drift-barrier hypothesis and mutation-rate evolution. *Proc. Natl. Acad. Sci. U. S. A.* **109**, 18488-18492 (2012).
9. E. Landolt, in *Bericht der Schweizerischen Botanischen Gesellschaft*. (1957), vol. 67, pp. 271-410.
10. P. Ziegler, K. Adelmann, S. Zimmer, C. Schmidt, K. J. Appenroth, Relative in vitro growth rates of duckweeds (Lemnaceae) - the most rapidly growing higher plants. *Plant Biol. (Stuttg)* **17 Suppl 1**, 33-41 (2015).
11. Y. L. Xu *et al.*, Species distribution, genetic diversity and barcoding in the duckweed family (Lemnaceae). *Hydrobiologia* **743**, 75-87 (2015).
12. M. Bog *et al.*, Genetic characterization and barcoding of taxa in the genera *Landoltia* and *Spirodela* (Lemnaceae) by three plastidic markers and amplified fragment length polymorphism (AFLP). *Hydrobiologia* **749**, 169-182 (2015).
13. See supplementary materials.
14. W. Wang *et al.*, The *Spirodela polyrhiza* genome reveals insights into its neotenous reduction fast growth and aquatic lifestyle. *Nature Communications* **5**, 3311 (2014).
15. A. McKenna *et al.*, The genome analysis toolkit: a MapReduce framework for analyzing next-generation DNA sequencing data. *Genome Res.* **20**, 1297-1303 (2010).
16. J. Cao *et al.*, Whole-genome sequencing of multiple *Arabidopsis thaliana* populations. *Nat. Genet.* **43**, 956-U960 (2011).
17. C. Jiang *et al.*, Environmentally responsive genome-wide accumulation of *de novo Arabidopsis thaliana* mutations and epimutations. *Genome Res.* **24**, 1821-1829 (2014).
18. A. F. Agrawal, M. C. Whitlock, Environmental duress and epistasis: how does stress affect the strength of selection on new mutations? *Trends Ecol. Evol.* **25**, 450-458 (2010).
19. C. Matsuba, D. G. Ostrow, M. P. Salomon, A. Tolani, C. F. Baer, Temperature, stress and spontaneous mutation in *Caenorhabditis briggsae* and *Caenorhabditis elegans*. *Biol. Lett.* **9**, 20120334 (2013).
20. A. Shibai *et al.*, Mutation accumulation under UV radiation in *Escherichia coli*. *Sci. Rep.* **7**, 14531 (2017).
21. E. M. Willing *et al.*, UVR2 ensures transgenerational genome stability under simulated natural UV-B in *Arabidopsis thaliana*. *Nat. Commun.* **7**, 13522 (2016).
22. H. Long *et al.*, Low base-substitution mutation rate in the germline genome of the ciliate *Tetrahymena thermophil*. *Genome Biol. Evol.* **8**, 3629-3639 (2016).
23. L. Klimes, J. Klimesov, R. Hendriks R, J.M. van Groenendael, H. d. Kroon, in *The ecology and evolution of clonal plants,* Kroon H, v. Groenendael, Eds. (Backhuys, Leiden, The Netherlands, 1997), pp. 1-29.
24. D. McKey, M. Elias, B. Pujol, A. Duputie, The evolutionary ecology of clonally propagated domesticated plants. *New Phytol.* **186**, 318-332 (2010).
25. A. Healey, A. Furtado, T. Cooper, R. J. Henry, Protocol: a simple method for extracting next-generation sequencing quality genomic DNA from recalcitrant plant species. *Plant Methods* **10**, 21 (2014).
26. M. Schubert, S. Lindgreen, L. Orlando, AdapterRemoval v2: rapid adapter trimming, identification, and read merging. *BMC Res. Notes* **9**, 88 (2016).

27. H. Li, R. Durbin, Fast and accurate short read alignment with Burrows-Wheeler transform. *Bioinformatics* **25**, 1754-1760 (2009).
28. H. Li *et al.*, The sequence alignment/map format and SAMtools. *Bioinformatics* **25**, 2078-2079 (2009).
29. M. A. DePristo *et al.*, A framework for variation discovery and genotyping using next-generation DNA sequencing data. *Nat. Genet.* **43**, 491-498 (2011).
30. G. A. Van der Auwera *et al.*, From FastQ data to high confidence variant calls: the genome analysis toolkit best practices pipeline. *Curr. Protoc. Bioinformatics* **43**, 11.10.11-11.10.33 (2013).
31. P. Cingolani *et al.*, A program for annotating and predicting the effects of single nucleotide polymorphisms, SnpEff: SNPs in the genome of *Drosophila melanogaster* strain w1118; iso-2; iso-3. *Fly (Austin)* **6**, 80-92 (2012).
32. P. Danecek *et al.*, The variant call format and VCFtools. *Bioinformatics* **27**, 2156-2158 (2011).
33. A. Raj, M. Stephens, J. K. Pritchard, fastSTRUCTURE: variational inference of population structure in large SNP data sets. *Genetics* **197**, 573-589 (2014).
34. B. Pfeifer, U. Wittelsburger, S. E. Ramos-Onsins, M. J. Lercher, PopGenome: an efficient Swiss army knife for population genomic analyses in R. *Mol. Biol. Evol.* **31**, 1929-1936 (2014).
35. C. W. Nelson, L. H. Moncla, A. L. Hughes, SNPGenie: estimating evolutionary parameters to detect natural selection using pooled next-generation sequencing data. *Bioinformatics* **31**, 3709-3711 (2015).
36. S. Purcell *et al.*, PLINK: a tool set for whole-genome association and population-based linkage analyses. *Am. J. Hum. Genet.* **81**, 559-575 (2007).
37. J. K. Pritchard, M. Przeworski, Linkage disequilibrium in humans: models and data. *Am. J. Hum. Genet.* **69**, 1-14 (2001).
38. K. M. Weiss, A. G. Clark, Linkage disequilibrium and the mapping of complex human traits. *Trends Genet.* **18**, 19-24 (2002).
39. J. A. Sved, Linkage disequilibrium and homozygosity of chromosome segments in finite populations. *Theor. Popul. Biol.* **2**, 125-141 (1971).
40. W. G. Hill, Estimation of effective population size from data on linkage disequilibrium. *Genetical Res.* **38**, 209-216 (1981).
41. K. G. Ardlie, L. Kruglyak, M. Seielstad, Patterns of linkage disequilibrium in the human genome. *Nat. Rev. Genet.* **3**, 299-309 (2002).
42. J. M. Flynn, F. J. Chain, D. J. Schoen, M. E. Cristescu, Spontaneous mutation accumulation in *Daphnia pulex* in selection free vs. competitive environments. *Mol. Biol. Evol.* **34**, 160-173 (2017).
43. S. Ossowski *et al.*, The rate and molecular spectrum of spontaneous mutations in *Arabidopsis thaliana*. *Science* **327**, 92-94 (2010).
44. J. T. Robinson *et al.*, Integrative genomics viewer. *Nat. Biotechnol.* **29**, 24-26 (2011).
45. H. Thorvaldsdottir, J. T. Robinson, J. P. Mesirov, Integrative genomics viewer (IGV): high-performance genomics data visualization and exploration. *Brief Bioinform.* **14**, 178-192 (2013).
46. L. Lopez-Maury, S. Marguerat, J. Bahler, Tuning gene expression to changing environments: from rapid responses to evolutionary adaptation. *Nat. Rev. Genet.* **9**, 583-593 (2008).
47. M. Lynch *et al.*, Genetic drift, selection and the evolution of the mutation rate. *Nat. Rev. Genet.* **17**, 704-714 (2016).
48. C. G. Feng *et al.*, Moderate nucleotide diversity in the Atlantic herring is associated with a low mutation rate. *eLife* **6**, e23907 (2017).

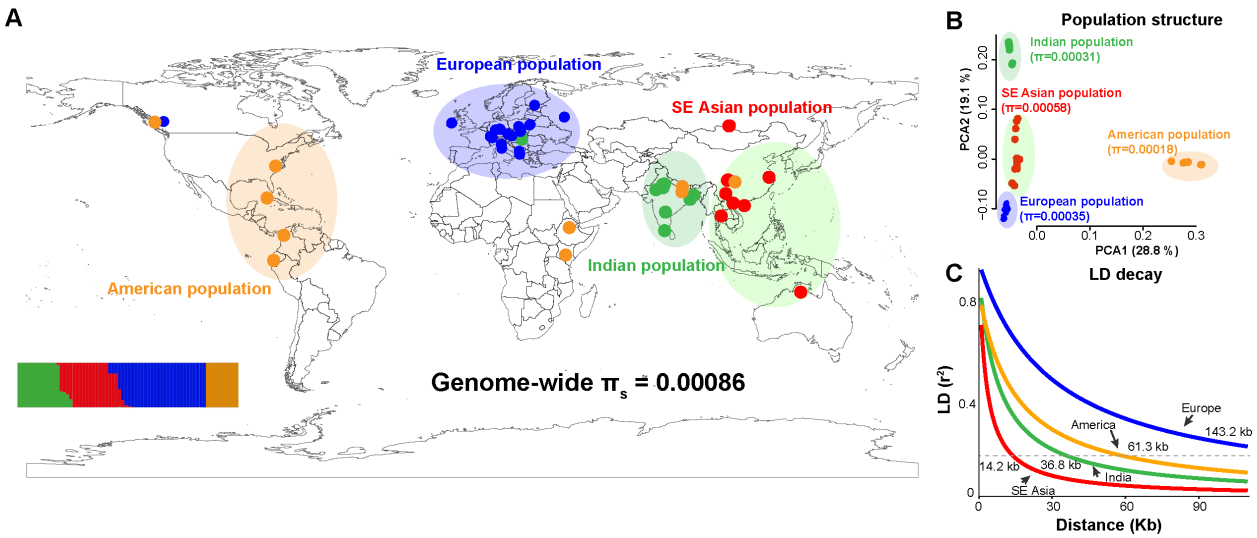

418

419 **Fig. 1. Genome-wide nucleotide diversity, population structure and linkage disequilibrium**

420 **in *S. polyrhiza*.** (**A**) Geographic distribution of the 68 sequenced samples, colored according to

421 population structure. The insert at the lower left corner shows the results from the STRUCTURE

422 analysis using genome-wide polymorphisms. Each colored line refers to an individual and the Y-

423 axis refers to the likelihood. Genome wide π_s refers to average pairwise nucleotide diversity at

424 synonymous sites. (**B**) Principal Coordinate Analysis (PCA) based on genome-wide nucleotide

425 diversity data. Average pairwise nucleotide diversity (π) calculated from all sites is shown for

426 each population. (**C**) Decay of linkage disequilibrium (LD) with physical distance in four

427 populations. The dashed line indicates an LD value of $r^2 = 0.2$, and the numbers refer to the

428 mean pairwise distance between sites at $r^2 = 0.2$.

429

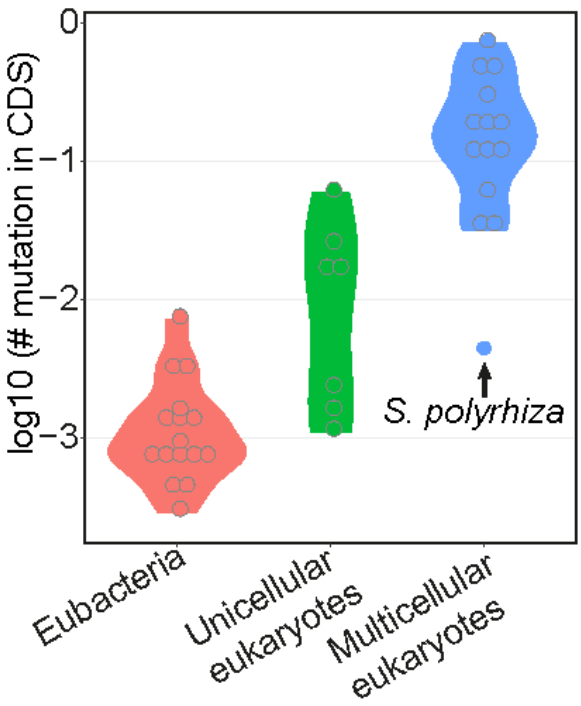

Fig. 2. Estimated mutation rates in protein-coding regions among different organisms. The $\log_{10}$-transformed number of mutations per base pair of protein-coding genome sequences (CDS) per generation is plotted for eubacteria, unicellular eukaryotes and multicellular eukaryotes, respectively. Each gray circle indicates the estimate for one species. The arrow highlights the mutation rate in *S. polyrhiza*. Except for the mutation rate in *S. polyrhiza*, the plotted data were extracted from previous studies (Table S3).

Table 1. Summary of the sequencing data and detected mutations.

Each row shows the sample information and number of verified mutations. Effective sites are estimated as the total number of sites with sufficient coverage for finding *de novo* variants using our pipeline. The mutation rate was calculated as μ = (number of mutations / sum of effective sites) / number of generations.

Sample ID	Treatment	# Mutations	Effective sites (Mb)	Average μ
A	Indoor	0	126.4	
E	Indoor	0	125.7	
I	Indoor	0	126.0	**<7.92E-11**
J	Indoor	0	126.4	
N	Indoor	0	125.9	
B	Outdoor-noUV	0	126.1	
G	Outdoor-noUV	**1**	126.3	
K	Outdoor-noUV	0	124.2	**7.92E-11**
O	Outdoor-noUV	0	125.9	
P	Outdoor-noUV	0	126.4	
C	Outdoor-UV	**1**	125.6	
D	Outdoor-UV	**1**	126.3	
L	Outdoor-UV	**1**	126.3	**2.38E-10**
M	Outdoor-UV	0	126.3	
Q	Outdoor-UV	0	126.0	

446 **Supplementary figures and tables.**

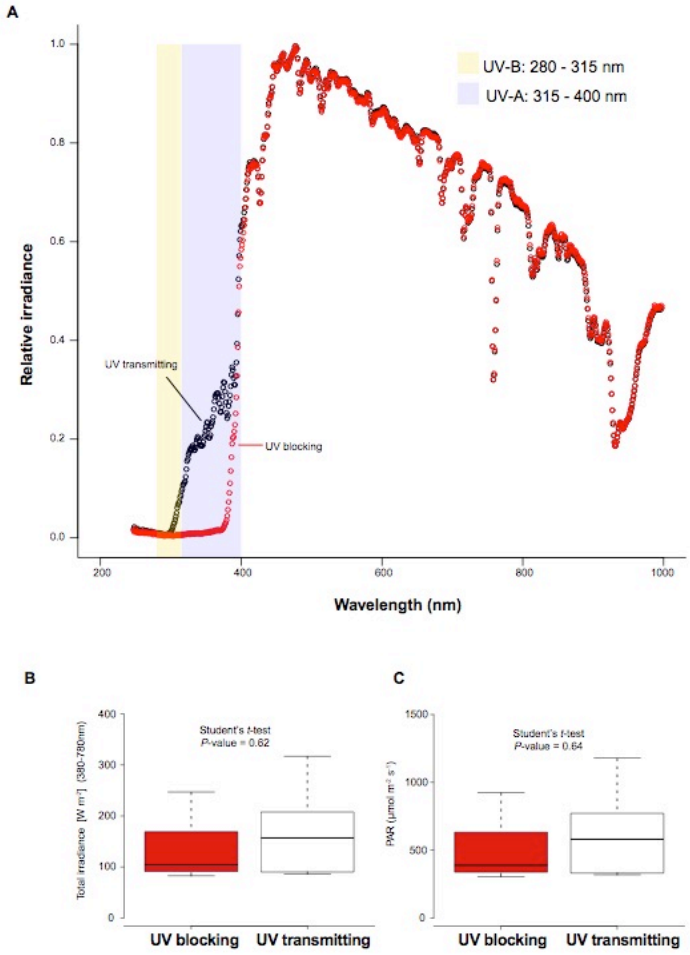

447

448 **Figure S1. Spectral properties of UV blocking and UV transmitting plexiglass covers.** A,
449 relative irradiance (irradiance / max irradiance per plate) in UV transmitting (GS 2458, $n = 9$)
450 and UV blocking (UV Gallery100, $n = 9$) plexiglass. B and C, total irradiance (B) and PAR (C)
451 did not differ between UV transmitting and UV blocking plexiglass ($n = 9$). The irradiance from
452 250 to 1000 nm, as well as total irradiance between 380 and 780 nm and photosynthetic active
453 radiation (PAR) between 400 and 700 nm were measured to assess the spectrum of the UV
454 transmitting and UV blocking types of plexiglass (Sandrock, Germany) that were used in the
455 mutation accumulation experiments.

456

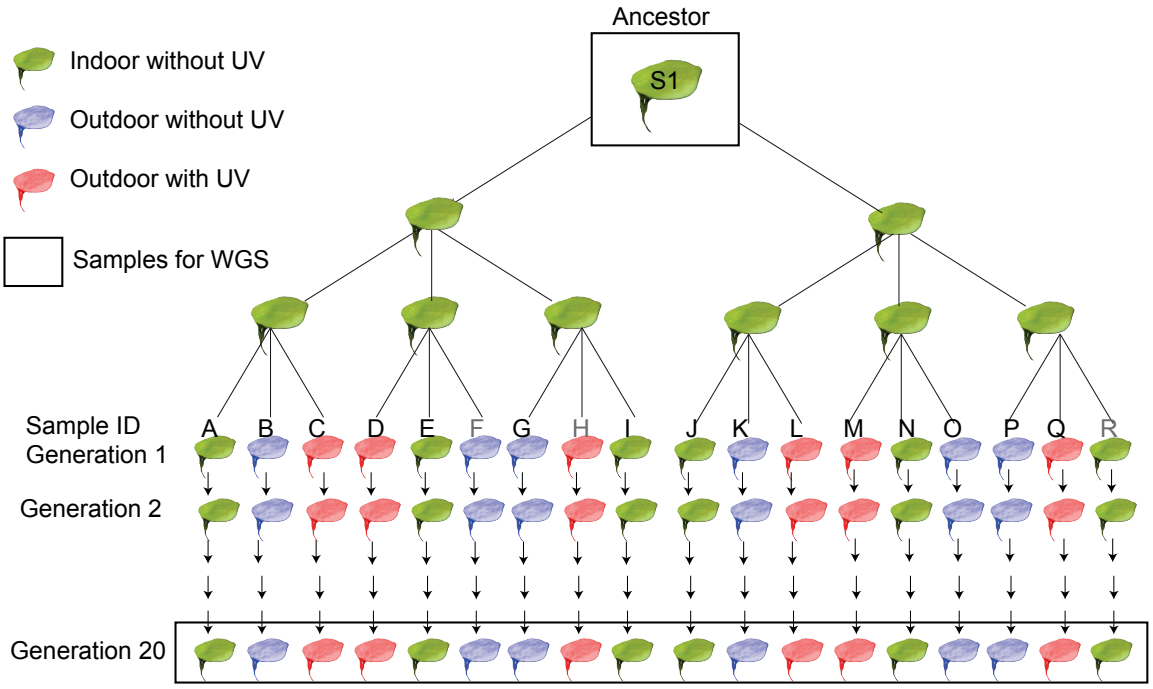

457

458 **Figure S2. Propagating scheme of the individuals for the mutation accumulation**

459 **experiments.** A single ancestor was used to propagate 18 individuals, which were then

460 propagated for 20 generations with a single-descendant approach. Among the 18 individuals

461 collected, three individuals (F, H and R, in gray color) were not included for the data analysis

462 due to their low sequencing depth. Each color represents a different treatment. Samples that were

463 used for sequencing are marked with a black box (bottom row).

464

Table S1. Sample and sequencing information of 68 *S. polyrhiza* genotypes. Mapped reads refer to all uniquely mapped reads, coverage was calculated based on the nuclear genome, and accession ID refers to the registered four-digit code of each genotype. The relatively low mapping rates from some samples were mainly due to non-plant DNAs.

Sample ID	Reads sequenced (million)	Mapped reads (million)	Mapping rate (%)	Coverage (X)	Accession ID	Continent	Country
Sp1	40.1	19.4	48.47	16.4	0040	Asia	China
Sp10	47.3	34.3	72.37	27.4	8790	America	Canada
Sp100	49.2	34.2	69.53	29.7	5525	Asia	Thailand
Sp101	46.5	32.8	70.44	26.8	5526	Asia	Thailand
Sp105	55.3	30.1	54.37	24.9	10F-IP-112	Europe	Switzerland
Sp106	52.7	37.1	70.33	30.7	S5	Europe	Switzerland
Sp11	49.3	33.2	67.38	28.9	9242	America	Ecuador
Sp12	39.9	29.9	75.05	23.7	9503	Asia	India
Sp13	48.6	38.1	78.34	32.9	9507	Asia	Russia
Sp14	47.1	33.2	70.58	28.5	9509	Europe	Germany
Sp15	41.7	33.4	80.09	27.5	9510	Africa	Mozambique
Sp16	48.4	36.8	76.10	31.8	9636	Asia	China
Sp17	50.0	38.5	77.15	32.1	9907	Asia	Bangladesh
Sp18	56.7	44.1	77.76	38.8	9511	Asia	Russia
Sp19	47.0	35.9	76.35	28.8	9925b	Asia	Bangladesh
Sp20	51.9	38.9	74.87	33.0	9625	Europe	Albania
Sp21	47.1	31.1	65.96	26.3	9500	Europe	Germany
Sp22	69.7	53.1	76.19	45.8	9628	Europe	Albania
Sp23	48.8	35.0	71.78	29.6	9618	Europe	Italy
Sp24	43.7	34.1	78.02	28.4	5523	Asia	China
Sp25	52.2	37.9	72.57	31.2	9351	Asia	Vietnam
Sp26	55.1	42.6	77.25	36.3	9633	Europe	Albania
Sp30	44.3	29.7	66.94	26.3	8442	Asia	India
Sp31	50.1	37.1	73.93	32.0	9514	Europe	Austria
Sp32	45.1	35.8	79.34	30.4	9505	America	Cuba
Sp34	49.2	33.6	68.29	28.0	9502	Europe	Ireland
Sp35	45.3	27.5	60.70	22.9	0109	Asia	China
Sp36	48.3	36.1	74.67	31.6	0092	Asia	China
Sp38	48.3	36.8	76.29	32.1	5521	Asia	China
Sp39	44.0	32.8	74.38	28.5	9650	Asia	India

Sp4	44.2	30.1	68.08	25.1	7498	America	USA
Sp40	53.5	36.7	68.47	32.7	9295	Asia	India
Sp41	43.7	35.7	81.76	30.4	9609	Europe	Poland
Sp42	52.2	35.8	68.53	29.4	9629	Europe	Albania
Sp43	49.4	28.3	57.39	24.4	9497	Asia	India
Sp45	45.1	36.1	79.98	30.7	9512	Asia	Russia
Sp46	50.6	39.8	78.60	33.1	9504	Asia	India
Sp47	48.1	26.1	54.29	21.6	9613	Europe	Poland
Sp48	45.7	28.2	61.74	23.6	9305	Asia	India
Sp5	40.4	25.0	61.85	21.6	7551	Asia	Australia
Sp50	44.1	35.9	81.51	29.7	0090	Asia	China
Sp51	48.1	26.6	55.27	22.0	9316	Asia	India
Sp53	41.6	28.1	67.65	22.7	9290	Asia	India
Sp54	42.1	25.6	60.83	21.1	8787	Asia	Nepal
Sp55	45.5	34.0	74.55	29.1	9610	Europe	Poland
Sp56	45.9	26.3	57.33	21.9	9256	Europe	Finland
Sp57	48.0	34.2	71.16	28.3	9333	Asia	China
Sp58	43.3	33.8	77.92	27.2	9560	Europe	Hungary
Sp59	44.9	35.2	78.26	29.4	9506	Asia	India
Sp61	43.7	32.0	73.09	26.8	0225	Asia	China
Sp62	46.0	19.6	42.54	16.5	9513	Europe	Czech Republic
Sp63	44.2	26.5	59.97	22.3	0013	Asia	Vietnam
Sp65	53.6	41.2	76.77	34.6	9413	Europe	Italy
Sp66	54.8	41.1	74.98	30.7	9622	Europe	Germany
Sp7	44.1	32.9	74.50	27.7	7674	Asia	Nepal
Sp71	49.5	27.4	55.26	24.0	9608	Europe	Poland
Sp72	50.4	29.0	57.59	23.4	5522	Asia	China
Sp77	55.2	43.1	78.14	37.3	9508	Europe	Poland
Sp78	47.1	33.6	71.41	29.3	9607	Europe	Switzerland
Sp79	49.2	35.4	71.94	30.9	5513	Europe	Germany
Sp8	43.7	34.6	79.04	28.9	8683	Africa	Kenya
Sp82	44.1	33.6	76.27	28.7	9649	Asia	India
Sp85	50.0	38.0	76.06	34.0	9192	America	Colombia
Sp87	55.6	39.6	71.28	34.9	9657	America	Canada
Sp89	58.3	41.6	71.30	37.2	0192	Asia	China
Sp9	40.8	29.1	71.33	25.0	8756	Africa	Ethiopia
Sp93	52.5	41.8	79.48	33.7	9346	Europe	Switzerland
Sp99	54.9	37.3	67.93	31.8	5524	Asia	Thailand

469

Table S2. Summary statistics of population genomics in *S. polyrhiza*. π referes to the estimated pairwise nucleotide diversity. π_a refers to the nucleotide diversity at non-synonymous sites and π_s refers to the nucleotide diversity at synonymous sites.

Summary statistics	Genome-wide π	π in coding regions	π in noncoding regions	Nonsyn. variants	Syn. variants	π_a	π_s	π_a/π_s
All populations combined	0.0013	0.00051	0.0014	14,191	8,865	0.00038	0.00086	0.44

Table S3. Summary of mutation rate and effective population size (N_e) estimates. Data is obtained from Lynch et al. 2016 (*47*), with a few updates (*48*). Mutation rate (μ) is listed as per generation per site. NA: not available. CDS: protein coding sequence. The estimated π from neutral sites is calculated as $D \times N_e \times \mu$, where D refers to 4 (diploid species) or 2 (haploid species).

Species	Group	μ	*Ne*	Genome size (Mb)	CDS size (Mb)	Mutations per CDS per generation	Estimated π from neutral sites
Apis mellifera	Multicellular eukaryotes	6.80E-09	NA	262.0	29.0	0.197	NA
Arabidopsis thaliana	Multicellular eukaryotes	6.95E-09	2.9E+05	119.7	42.1	0.292	0.00806
Caenorhabditis briggsae	Multicellular eukaryotes	1.33E-09	2.7E+05	104.0	24.1	0.032	0.00144
Caenorhabditis elegans	Multicellular eukaryotes	1.45E-09	5.4E+05	100.3	25.0	0.036	0.00313
Daphnia pulex	Multicellular eukaryotes	5.69E-09	8.3E+05	250.0	30.2	0.172	0.01889
Drosophila melanogaster	Multicellular eukaryotes	5.17E-09	8.6E+05	168.7	23.2	0.120	0.01778
Heliconius melpomene	Multicellular eukaryotes	2.90E-09	2.1E+06	273.8	39.1	0.113	0.02436
Homo sapiens	Multicellular eukaryotes	1.35E-08	2.1E+04	3300.0	36.5	0.493	0.00113
Mus musculus	Multicellular eukaryotes	5.40E-09	1.8E+05	2717.0	35.5	0.192	0.00389
Oryza sativa	Multicellular eukaryotes	7.10E-09	5.3E+04	389.0	101.3	0.719	0.00151
Pan troglodytes	Multicellular eukaryotes	1.20E-08	2.9E+04	3524.0	37.2	0.446	0.00139
Pristionchus pacificus	Multicellular eukaryotes	2.00E-09	1.8E+06	169.7	29.7	0.059	0.01440
Clupea harengus	Multicellular eukaryotes	2.00E-09	4.0E+05	850.0	57.6	0.115	0.00320
Spirodela polyrhiza	**Multicellular eukaryotes**	**2.38E-10**	9.0E+05	**158.0**	**17.4**	**0.004**	0.00086
Chlamydomonas reinhardtii	Unicellular eukaryotes	3.80E-10	4.3E+07	111.1	39.2	0.015	0.03268
Neurospora crassa	Unicellular eukaryotes	4.10E-09	1.8E+06	38.6	14.5	0.059	0.01476
Paramecium tetraurelia	Unicellular eukaryotes	1.94E-11	1.0E+08	72.1	56.8	0.001	0.00776
Plasmodium falciparum	Unicellular eukaryotes	2.08E-09	3.5E+05	22.9	12.1	0.025	0.00146
Saccharomyces cerevisiae	Unicellular eukaryotes	2.63E-10	7.8E+06	12.5	8.7	0.002	0.00410
Schizosaccharomyces pombe	Unicellular eukaryotes	2.17E-10	1.4E+07	19.6	7.2	0.002	0.00608

Trypanosoma brucei	Unicellular eukaryotes	1.38E-09	5.3E+06	26.1	13.2	0.018	0.02926
Agrobacterium tumefaciens	Eubacteria	2.92E-10	3.4E+08	5.7	5.0	0.001	0.19856
Bacillus subtilis	Eubacteria	3.35E-10	6.1E+07	4.3	3.6	0.001	0.04087
Burkholderia cenocepacia	Eubacteria	1.33E-10	2.5E+08	7.7	6.7	0.001	0.06650
Deinococcus radiodurans	Eubacteria	4.99E-10	NA	3.3	2.9	0.001	NA
Escherichia coli	Eubacteria	2.00E-10	1.8E+08	4.6	3.9	0.001	0.072
Helicobacter pylori	Eubacteria	1.90E-09	4.0E+07	1.7	1.5	0.003	0.152
Mesoplasma florum	Eubacteria	9.78E-09	1.1E+06	0.8	0.7	0.007	0.022
Mycobacterium smegmatis	Eubacteria	5.27E-10	NA	7.0	6.5	0.003	NA
Mycobacterium tuberculosis	Eubacteria	1.95E-10	NA	4.4	4.0	0.001	NA
Pseudomonas aeruginosa	Eubacteria	7.92E-11	2.1E+08	6.5	5.9	0.000	0.0333
Salmonella enterica	Eubacteria	1.74E-10	3.5E+08	4.9	4.0	0.001	0.1218
Salmonella typhimurium	Eubacteria	1.52E-10	NA	4.9	4.3	0.001	NA
Staphylococcus epidermidis	Eubacteria	7.40E-10	3.5E+07	2.6	2.1	0.002	0.0518
Thermus thermophilus	Eubacteria	1.38E-10	2.3E+08	2.1	2.1	0.000	0.0635
Vibrio cholerae	Eubacteria	1.15E-10	4.8E+08	3.9	3.4	0.000	0.1104
Vibrio fischeri	Eubacteria	2.08E-10	NA	4.3	3.7	0.001	NA

482

483

484 **Table S4. Pairwise Fst between four population groups. The number of sequenced**
485 **individuals is listed in bracket.**
486

Population	India (13)	SE Asia (18)	Europe (27)	America (10)
India (13)	/	/	/	/
SE Asia (18)	0.47	/	/	/
Europe (27)	0.65	0.35	/	/
America (10)	0.82	0.67	0.79	/

487

Table S5. Summary of nucleotide diversity (ND) in *S. polyrhiza*. The summary statistics of nucleotide diversity are shown separately for each chromosome. Ti/Tv: Transition to Transversion ratio. Fst is calculated among all four populations. π: average pairwise nucleotide diversity from all sites.

Chr ID	Size (bp)	Ti/ Tv	Fst	π in India	π in SE Asia	π in Europe	π in America
ChrS01	11466534	2.16	0.67	0.00026	0.00050	0.00030	0.00018
ChrS02	8941172	2.21	0.67	0.00026	0.00056	0.00033	0.00015
ChrS03	8796147	2.23	0.73	0.00026	0.00061	0.00034	0.00014
ChrS04	8491500	2.18	0.69	0.00025	0.00051	0.00035	0.00011
ChrS05	8389602	2.28	0.66	0.00042	0.00062	0.00039	0.00021
ChrS06	8130874	2.24	0.71	0.00023	0.00058	0.00033	0.00018
ChrS07	8107549	2.30	0.70	0.00041	0.00060	0.00024	0.00017
ChrS08	7340019	2.09	0.68	0.00028	0.00049	0.00027	0.00014
ChrS09	7208038	2.19	0.68	0.00033	0.00055	0.00035	0.00017
ChrS10	7041313	2.25	0.66	0.00036	0.00057	0.00042	0.00022
ChrS11	6552830	2.20	0.71	0.00026	0.00054	0.00029	0.00017
ChrS12	5946178	2.18	0.62	0.00037	0.00067	0.00043	0.00024
ChrS13	5476630	2.20	0.70	0.00024	0.00047	0.00036	0.00016
ChrS14	5103705	2.19	0.63	0.00034	0.00061	0.00039	0.00025
ChrS15	4726429	2.38	0.65	0.00034	0.00061	0.00038	0.00019
ChrS16	4623610	2.40	0.72	0.00027	0.00070	0.00029	0.00020
ChrS17	4564609	2.30	0.67	0.00038	0.00069	0.00037	0.00016
ChrS18	4370269	2.31	0.71	0.00030	0.00056	0.00040	0.00013
ChrS19	3727809	2.26	0.65	0.00038	0.00058	0.00039	0.00016
ChrS20	3541257	2.11	0.69	0.00030	0.00062	0.00029	0.00020

Table S6. Summary of the information of the sequencing coverage for the mutation accumulation experiments. The coverage was calculated based on all properly mapped reads after removing the PCR duplicates. All sample IDs refer to the samples showed in Figure S2, except sample V, which refers to the ancestor (labeled as S1 in Figure S2).

Sample ID	Coverage (X)
A	29
B	27
C	30
D	36
E	22
G	33
I	34
J	32
K	20
L	24
M	34
N	28
O	23
P	27
Q	23
V	29

Table S7. Detailed information for all putative MA variants. Most of the putative variants were loss-of-heterozygosity (LOH) mutations and located in clusters, likely due to false positives. The variants that were validated using Sanger sequencing are highlighted in red, which are all located in non-coding region. AD refers to the number of reads supporting reference and alternative alleles, respectively.

Chr	Location	Sample	AD	Reference	Variant	Type	Variant class
ChrS01	6301633	B	9,0	C	T	SnpCluster	LOH in Offspring
ChrS01	6778840	G	4,21	CT	C	InDel	LOH in Ancestor
ChrS01	9852279	M	0,12	A	T	SnpCluster	LOH in Offspring
ChrS02	6163960	B	9,0	C	CACCA	InDel;SnpCluster	LOH in Offspring
ChrS02	6830760	A	0,15	A	AG	InDel;SnpCluster	LOH in Offspring
ChrS03	1281216	I	3,26	TG	T	InDel	LOH in Ancestor
ChrS03	6136639	G	3,19	AT	A	InDel;SnpCluster	LOH in Ancestor
ChrS04	1185527	I	12,0	G	C	InDel;SnpCluster	LOH in Offspring
ChrS04	3829456	O	3,23	T	TA	InDel	LOH in Ancestor
ChrS04	6079575	D	0,18	C	T	SnpCluster	LOH in Offspring
ChrS04	8490307	C	14,8	C	A	Snp	Point-Mutation
ChrS05	3677104	P	3,23	A	AT	InDel	LOH in Ancestor
ChrS05	6844652	P	22,0	A	T	InDel;SnpCluster	LOH in Offspring
ChrS05	6844656	P	20,0	A	G	InDel;SnpCluster	LOH in Offspring
ChrS06	1632818	D	26,9	C	T	Snp	Point-Mutation
ChrS06	5745754	B	18,0	A	G	InDel;SnpCluster	LOH in Offspring
ChrS06	5785368	A	0,8,3	CCTCTCTC TCTCTCT	C,CCTCTC TCTCTCT	InDel	LOH in Offspring
ChrS07	1417860	C	10,0	TATGATG ATGATG	T	InDel	LOH in Offspring
ChrS07	6027616	I	11,0	T	TTCTCTCT CTCTCTCT CTC	InDel	LOH in Offspring
ChrS08	26	B	11,0	A	C	SnpCluster	LOH in Offspring
ChrS08	293223	Q	25,7	G	C	SnpCluster	Point-Mutation
ChrS08	3298264	L	18,0	C	CCT	InDel	LOH in Offspring
ChrS08	3298264	D	18,0	G	A	InDel	LOH in Offspring
ChrS08	5474787	J	3,28	A	AT	InDel;SnpCluster	LOH in Ancestor
ChrS08	6346309	L	17,7	G	A	Snp	Point-Mutation
ChrS09	654554	I	41,13	G	C	SnpCluster	Point-Mutation
ChrS09	732653	L	0,10	TC	T	InDel;SnpCluster	LOH in Offspring
ChrS09	4187399	G	25,8	C	T	Snp	Point-Mutation

ChrS10	316751	A	11,0	A	AG	InDel	LOH in Offspring
ChrS10	832372	P	0,26	C	T	InDel;SnpCluster	LOH in Offspring
ChrS10	1666647	E	0,11	T	C	SnpCluster	LOH in Offspring
ChrS10	1758399	J	10,0	A	G	SnpCluster	LOH in Offspring
ChrS10	2446237	D	12,0	A	C	SnpCluster	LOH in Offspring
ChrS10	2649843	J	28,0	T	TCTG	InDel;SnpCluster	LOH in Offspring
ChrS10	6671568	B	9,0	G	A	SnpCluster	LOH in Offspring
ChrS11	104836	L	3,16	C	CA	InDel	LOH in Ancestor
ChrS11	621931	O	3,23	G	GA	InDel;SnpCluster	LOH in Ancestor
ChrS11	2700514	G	0,11	AG	A	InDel;SnpCluster	LOH in Offspring
ChrS11	2915562	C	17,0	C	T	InDel;SnpCluster	LOH in Offspring
ChrS11	3702448	G	9,0	G	A	Snp	LOH in Offspring
ChrS12	2385087	J	3,13	GA	G	InDel;SnpCluster	LOH in Ancestor
ChrS12	3270743	G	0,16	T	A	InDel	LOH in Offspring
ChrS12	5630221	N	12,0	T	C	InDel;SnpCluster	LOH in Offspring
ChrS13	711097	B	3,28	G	GA	InDel	LOH in Ancestor
ChrS13	4947823	I	9,0	CAGAGAG AGAGAG	C	InDel	LOH in Offspring
ChrS14	1204760	P	13,0	G	A	SnpCluster	LOH in Offspring
ChrS14	1802774	M	0,27	C	T	InDel;SnpCluster	LOH in Offspring
ChrS14	2063032	P	47,0	A	T	SnpCluster	LOH in Offspring
ChrS14	2211208	L	37,0	T	A	SnpCluster	LOH in Offspring
ChrS14	4587419	Q	0,15	C	T	Snp	LOH in Offspring
ChrS14	4633108	Q	15,0	T	G	SnpCluster	LOH in Offspring
ChrS14	4691382	O	14,0	G	GGAGA	InDel	LOH in Offspring
ChrS15	583186	E	7,3	G	T	Snp	Point-Mutation
ChrS15	1247924	E	18,0	G	A	SnpCluster	LOH in Offspring
ChrS15	2926508	P	0,12	TC	T	InDel;SnpCluster	LOH in Offspring
ChrS15	4459454	P	4,14	A	AT	InDel;SnpCluster	LOH in Ancestor
ChrS15	4478521	I	28,9	G	A	Snp	Point-Mutation
ChrS17	135160	G	4,12	TG	T	InDel	LOH in Ancestor
ChrS17	3461404	N	0,20	C	T	InDel;SnpCluster	LOH in Offspring
ChrS17	4562113	G	4,17	C	CAA	InDel	LOH in Ancestor
ChrS19	742326	B	3,13	C	CT	InDel	LOH in Ancestor
ChrS19	1262617	N	0,23	G	T	InDel;SnpCluster	LOH in Offspring
ChrS19	1933754	P	11,0	T	C	InDel;SnpCluster	LOH in Offspring
ChrS20	25868	B	10,0	T	C	SnpCluster	LOH in Offspring
ChrS20	146748	I	17,0	T	C	SnpCluster	LOH in Offspring
ChrS20	2505484	N	4,16	TA	T	InDel;SnpCluster	LOH in Ancestor
ChrS20	2782126	M	9,0	A	C	SnpCluster	LOH in Offspring
ChrS20	3148831	J	0,10	G	C	InDel;SnpCluster	LOH in Offspring

ChrS20	3419412	L	3,24	A	AT	InDel	LOH in Ancestor
pseudo0	1904325	A	3,24	A	AT	InDel	LOH in Ancestor
pseudo0	3287661	D	3,27	C	CT	InDel	LOH in Ancestor
pseudo0	4251867	G	43,11	T	C	SnpCluster	Point-Mutation
pseudo0	5340142	B	16,0	T	C	SnpCluster	LOH in Offspring
pseudo0	5932673	N	11,0	T	C	InDel;SnpCluster	LOH in Offspring
pseudo0	7117967	I	3,19	C	CT	InDel;SnpCluster	LOH in Ancestor
pseudo0	9320040	D	13,0	T	A	Snp	LOH in Offspring
pseudo0	9589514	Q	20,13	T	C	SnpCluster	Point-Mutation
pseudo0	9589529	Q	23,11	C	G	SnpCluster	Point-Mutation
pseudo0	9589541	Q	25,8	G	C	SnpCluster	Point-Mutation
pseudo0	9596763	P	10,4	T	C	SnpCluster	Point-Mutation
pseudo0	10338194	N	17,0	A	T	SnpCluster	LOH in Offspring
pseudo0	10338200	N	19,0	T	C	SnpCluster	LOH in Offspring
pseudo0	10338207	N	17,0	T	C	SnpCluster	LOH in Offspring
pseudo0	10510028	M	6,4	C	T	SnpCluster	Point-Mutation
pseudo0	10770049	C	15,0	C	CCCA	InDel;SnpCluster	LOH in Offspring
pseudo0	11240888	I	11,0	A	AGG	InDel;SnpCluster	LOH in Offspring

509 **Table S8. Primer information for validating the variants.** All primers that were used for
510 validating the candidate variants are shown. Primer sequence information is shown in forward
511 (F) and reverse (R). The validation results are indicated in bold text.

Locus	Primer sequences	Sample ID	Locus Info	Location	Validation
SpMR02	F: TGATGGCTGCCTACTCTTGG, R: CCAGGTCAACGTCAAAGAAGA	G	SNPCluster	ChrS03_6136639	False positive
SpMR03	F:ATTATGGGCTTACCCCGACC, R:TTTCTGTAGGCCATGTCGAAG	I	SNPCluster	ChrS04_1185527	False positive
SpMR04	F:AGTCGAAGAACAACGCTGAC, R:CCTGTCACGATGGGTTTTAGT	O	InDel	ChrS04_3829456	False positive
SpMR05	**F:ACCAGTGCTGCAATGATTTTG, R:GGTGGATTGACCTTCTTGCAT**	**C**	**SNP**	**ChrS04_8490307**	**PASS**
SpMR06	F:AAGGGGTTTGGTAATTCGGG, R:TTGGGGGCGATTAACAGATG	P	InDel	ChrS05_3677104	False positive
SpMR07	**F:ATAAAGTTTCGGCTTTGCGG, R:ACTAAACCCGCCACCTTAAC**	**D**	**SNP**	**ChrS06_1632818**	**PASS**
SpMR08	F:CATGGCGGATGTGAGCATTT, R:AGGGAACCCCAATCCAAGGT	C	InDel	ChrS07_1417860	False positive
SpMR10	F:GACGTCGCATTTCATGATGG, R:CATCTGATCCGAAGAGGGC	Q	SNPCluster	ChrS08_293223	False positive
SpMR11	F:TTCAAGCATTGACTTTATGAGCC, R:AAGGTGAGGGAGAAAACGATG	J	SNPCluster	ChrS08_5474787	False positive
SpMR12	F:GATAGGAGGGAAAGCGACAG, R:CGAACCTTCTTGTGGTCGAA	L	InDel	ChrS08_2768334	False positive
SpMR13	F:AGCATCGGTTATGATCCAGC, R:AATGTCTTCAGAGAACCGCC	D	InDel	ChrS08_3298264	False positive
SpMR14	**F:GATGGGGAGATATGTGAAGCA, R:CGAATGAACTAAGCCCCTGTA**	**L**	**SNP**	**ChrS08_6346309**	**PASS**
SpMR15	F:GGTTCTCACAGACCCAAATCT, R:GATGTACACGGGCAACTACG	I	SNPCluster	ChrS09_654554	False positive
SpMR16	**F:AGAGGTGTAAAGACTTATTTCGCT, R:TGGTTAGTTGAAGTAGAATGACTTT**	**G**	**SNP**	**ChrS09_4187399**	**PASS**
SpMR17	F:CATCATTTCCAAGGTCAACGG, R:CGGATTCGGATACAAAGTGG	D	SNPCluster	ChrS10_2446237	False positive
SpMR18	F:AGTCGGAAAAATGTGACCCAG, R:CACGCCAGTCCAAGAAACTC	P	SNPCluster	ChrS10_832372	False positive
SpMR19	F:ATGACCACCAAAGTTGACCC, R:AATCGCCTGAAGAACAGACC	A	InDel	ChrS10_316751	False positive
SpMR20	F:ACCGAGTTTAGTCCCACATC, R:TTCCATCCCTTCTCCAACATT	C	SNPCluster	ChrS11_2915562	False positive
SpMR21	F:GACCTTCCTCTCAGGTTCTCT, R:GGTCCACCATATCCGTAGCA	O	SNPCluster	ChrS11_621931	False positive
SpMR22	F:CCGTCATCCAGAGCCATTTC, R:CTAGTCCACAGGAGAAGCGA	L	InDel	ChrS11_104836	False positive
SpMR23	F:AGTAGTCTGGAGCCGGTTTT, R:TGTGGTCACCTCTTTCAACC	J	SNPCluster	ChrS12_2385087	False positive
SpMR24	F:TCGCCATCTCATTGGTTGTG, R:AACACGCTCAGTTCGTCATC	N	SNPCluster	ChrS12_5630221	False positive
SpMR25	F:TTGCTTTGTTATGTGCATCCTT, R:CAACGTGACATAAGTGTGAGC	G	InDel	ChrS12_3270743	False positive

SpMR26	F:AGAAATCCTCTTGTGGACCC, R:AGAAGGTGACTAGGGCCAG	I	InDel	ChrS13_4947823	False positive
SpMR27	F:TAACCAAGAATTTCATGACGACAAA, R:TCATCCACGATCGGAAAACAC	B	InDel	ChrS13_711097	False positive
SpMR28	F:CACTGAAATCCTTGCTGGCT, R:TTCAAGTGGATCGTGAGAGG	M	SNPCluster	ChrS14_1802774	False positive
SpMR29	F:AGATCGCCGTCTCTCAGC, R:GATCTGCGACACAACCAAGA	Q	SNPCluster	ChrS14_4633108	False positive
SpMR30	F:AACAGACAACTGAACCATACG, R:AATGAACCCCAATACCCACC	Q	SNP	ChrS14_4587419	False positive
SpMR31	F:TCCTTGAGATAGAGGCAGTCC, R:TGATAATGTGCGGGCAAAAC	O	InDel	ChrS14_4691382	False positive
SpMR32	F:GCAAACATCTGCACTACAAGTTA, R:CGTATCACCTGCCGAAGAAG	E	SNPCluster	ChrS15_1247924	False positive
SpMR33	F:ACAATGGGTTGGACTCCCTAA, R:CTCCTAGAACGCCAACAGAG	I	SNP	ChrS15_4478521	False positive
SpMR34	F:CGCCATCCAAAAGGTCTACG, R:TAGAGCAGGGCACAGATCG	E	SNP	ChrS15_583186	False positive
SpMR35	F:TTACAGTCTCGACGCTCTCT, R:CTGGCCTCACATTACACGG	N	SNPCluster	ChrS17_3461404	False positive
SpMR36	F:TTCTGCCCACTTGAGAGGTA, R:TGATGCTTATGGTCCGCTTC	N	SNPCluster	ChrS19_1262617	False positive
SpMR37	F:CGCTGTTCTGAGTGTTTTCC, R:ACATACCCCACCCAAAGAGA	N	SNPCluster	ChrS20_2505484	False positive
SpMR38	F:AGGTTTCCAACGAAAGACGA, R:GCAGCCGTTAAGTTCCGAT	J	SNPCluster	ChrS20_3148831	False positive
SpMR39	F:TGTAGTGGTGATGGTGGCTA, R:TAGGAAGGTTAAAACTTAGGGCT	N	SNPCluster	pseudo0_10338194	False positive
SpMR40	F:GGCAGTCTAGTTGTGTTGAGT, R:GACGCTAATGCAACATCCACC	N	SNPCluster	pseudo0_10338200	False positive
SpMR41	F:AGATGTGGGCAGTCTAGTTGT, R:ACTGACGCTAATGCAACATCC	N	SNPCluster	pseudo0_10338207	False positive
SpMR42	F:TCCCGGTCAAGATCGTCAT, R:AGAAGATGTATTCCCAGCCC	M	SNPCluster	pseudo0_10510028	False positive
SpMR43	F:CAGTCGCCAGATGAGGGAAT, R:GTTGCCGTGAAAAGCACTAAT	C	SNPCluster	pseudo0_10770049	False positive
SpMR44	F:GGTCCCCGACTTCACGATT, R:GCCTTGGTTTCCTCGCATT	G	SNPCluster	pseudo0_4251867	False positive
SpMR45	F:AGAGTGAAGAGCGACATCCA, R:CTTCAACACCCAGAAGAAGC	B	SNPCluster	pseudo0_5340142	False positive
SpMR46	F:AACATAGAGGAAGGCCGTGA, R:CTTCCTGATGGGTTCGGTTC	I	SNPCluster	pseudo0_7117967	False positive
SpMR47	F:AATCGGAGGAACCCATCTCG, R:GGAAAGAGTGGCGTTGTATG	Q	SNPCluster	pseudo0_9589514	False positive
SpMR48	F:TGTGCTTCTTGACCTCGAAC , R:AACATCATCCTGTCCGGGTA	Q	SNPCluster	pseudo0_9589529	False positive

516

517 **External Dataset 1. Annotation of SNPs at the gene level.** The total number of SNPs that were
518 found in each gene is listed according to the predicted effects.

519

520 **External Dataset 2. Climate and light spectrum information in Jena (Germany), at the**
521 **place where the outdoor mutation accumulation experiments were performed.** Ambient
522 temperature, global radiation, PAR radiation and the UV spectrum are shown hourly.

523